
On the Laplace Approximation as Model Selection Criterion for Gaussian Processes

Andreas Besginow¹ Jan David Hüwel² Thomas Pawellek Christian Beecks² Markus Lange-Hegermann¹

Abstract

Model selection aims to find the best model in terms of accuracy, interpretability or simplicity, preferably all at once. In this work, we focus on evaluating model performance of Gaussian process models, i.e. finding a metric that provides the best trade-off between all those criteria. While previous work considers metrics like the likelihood, AIC or dynamic nested sampling, they either lack performance or have significant runtime issues, which severely limits applicability. We address these challenges by introducing multiple metrics based on the Laplace approximation, where we overcome a severe inconsistency occurring during naive application of the Laplace approximation. Experiments show that our metrics are comparable in quality to the gold standard dynamic nested sampling without compromising for computational speed. Our model selection criteria allow significantly faster and high quality model selection of Gaussian process models.

1. Introduction

Turning data into knowledge frequently requires inferring descriptive models which capture the major data characteristics. In particular in the domain of data science (and engineering), a common challenge lies in identifying an appropriate descriptive Machine Learning (ML) model that effectively learns interpretable information based on a given dataset without overfitting and underfitting.

When faced with small datasets, Gaussian processes (GPs) have become the preferred method for flexibly and interpretably modeling complex patterns in regression tasks. The interpretability and transparency offered by GPs can be attributed to the selection of a covariance function (also often called kernels), which possesses the ability to capture a

wide array of structures arising from diverse domains such as geometry (Borovitskiy et al., 2020), symmetry (Holderrrieth et al., 2021), harmonic analysis (Lázaro-Gredilla et al., 2010), or differential equations (Besginow & Lange-Hegermann, 2022; Alvarez et al., 2009; Härkönen et al., 2023). These covariance functions induce a strong prior that result in reasonable models even in the case of scarce data.

In cases where no such prior knowledge can be induced for covariance functions, one can resort to kernel search algorithms (Duvenaud et al., 2013; Berns et al., 2022; Hüwel et al., 2021) whose goal is selecting the best covariance function w.r.t. a given performance measure. These methods generally follow an iterative process to construct a descriptive covariance function from a set of base kernels and operations for a given regression data set. To ensure a good fit between model and data, kernel searches utilize different performance measures to evaluate the constructed models (Duvenaud et al., 2013; Kim & Teh, 2018). In the interest of interpretability, covariance functions with a minimal number of operands (e.g. summands) are generally preferred.

Most covariance functions come with (hyper)parameters. The values of hyperparameters are usually determined reliably by maximizing the Marginal Log Likelihood (MLL) $\log p(y|X, \theta)$ of the Gaussian likelihood (Rasmussen & Williams, 2006). So, inside of a single parametrized class of kernels, it is possible to identify the most suitable *parametrization* for a model. However, identifying the most suitable *class of kernels* purely from data remains a challenging task.

The gold standard for GP model selection is the computation of the model evidence $\mathcal{Z} = p(y|X) = \int p(y|X, \theta)p(\theta) d\theta$, which necessitates the challenging task of marginalizing over the hyperparameters θ . Achieving a high-quality approximation of this integral requires computationally intensive methods (cf. Figure 4) such as dynamic nested sampling (Skilling, 2006). However, to enhance computational efficiency, more approximate techniques are often employed, such as the MLL, the Akaike Information Criterion (AIC) or the Bayesian Information Criterion (BIC). Though, while the MLL is commonly utilized for hyperparameter fitting, it tends to overfit when used as a model selection criterion, as it never penalizes superfluous parameters. To address this

¹University of Applied Sciences and Arts, Lemgo, Germany
²University of Hagen, Hagen, Germany. Correspondence to: Andreas Besginow <andreas.besginow@th-owl.de>.

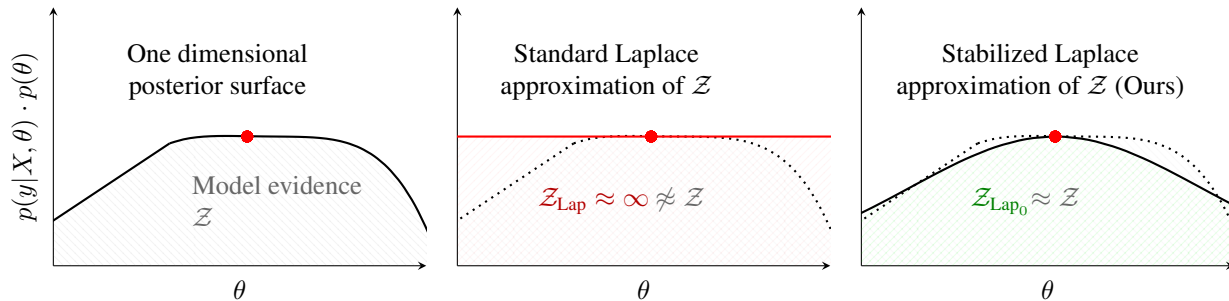


Figure 1. A conceptual visualization of the inconsistency when naively applying the Laplace approximation and one of our suggested variants. **Left:** The posterior over parametrizations θ , with a degenerate local extremum (red dot). The model evidence \mathcal{Z} is the gray shaded area. **Middle:** Naive application of the Laplace approximation around the optimum with infinitely large model evidence approximation $\mathcal{Z}_{\text{Lap}} \approx \infty \not\approx \mathcal{Z}$ overlaid in red. **Right:** Application of our stabilized Laplace (Lap₀) around the optimum with model evidence approximation $\mathcal{Z}_{\text{Lap}_0} \approx \mathcal{Z}$ overlaid in green.

limitation, AIC penalizes the number of parameters added to the MLL, thus mitigating overfitting. Alternatively, BIC aims to recover the original model and therefore imposes a larger penalty dependent on both the number of parameters and the number of data points (Burnham & Anderson, 2004; Burnham et al., 1998). Both of these approximations only take the number of hyperparameters and data points into account, and hence are rather crude.

In this study, we introduce a novel collection of model selection criteria for GPs that are not only computationally efficient but also yield robust performance. These criteria derive from the Laplace approximation of the parameter posterior to compute the model evidence integral (Bishop, 2006; Jaynes, 2003). While the Laplace approximation has been used to train GP hyperparameters or estimate the posterior predictive distribution (Li et al., 2023; Flaxman et al., 2015; Kuss & Rasmussen, 2005; Zilber & Katzfuss, 2021; Hartmann & Vanhatalo, 2019), to the best of our knowledge, this paper is the first to use Laplace approximation to compare the GP model evidence *between model classes*.

For this use case, we identify severe inconsistencies when naively applying the Laplace approximation where adding superfluous parameters improves the model evidence. To address these inconsistencies, we introduce variants of the Laplace approximation, by bounding the eigenvalues of the Hessian. Using our variants of the Laplace approximations prevents that additional parameters contribute positively to the model evidence, without significant contributions to the model fit. We illustrate the extreme case of these inconsistencies in Figure 1, where we mitigate the infinitely large approximation of the model evidence \mathcal{Z} , due to naive application of the standard Laplace approximation, using our Laplace approximations.

We show in experiments that our Laplace approximations perform as good as dynamic nested sampling while retaining

a small runtime. Additionally, in kernel search experiments we show how our different Laplace approximations have different strengths with respect to test performance and recognition of the underlying model.

The core contributions of this paper are as follows¹.

- We introduce new model selection criteria, based on the Laplace approximation, which mitigate the original inconsistency coming with naive application of the Laplace approximation
- We show that our criteria are comparable in approximation of the model evidence to dynamic nested sampling and offer similar interpretability as dynamic nested sampling, all while having a neglectable runtime
- In kernel search experiments we show the superiority of our Laplace approximations in predicting the model evidence of models, compared to the state of the art

2. Preliminaries

2.1. Gaussian Processes

A GP $g = \mathcal{GP}(\mu, k)$ is a stochastic process where every finite set of realizations at the points x_i are jointly Gaussian (Rasmussen & Williams, 2006). Such a GP is characterized by its mean function $\mu : \mathbb{R}^d \rightarrow \mathbb{R} : x \mapsto \mathbb{E}(g(x))$ (often set to zero) and its positive semi-definite covariance function (or kernel) $k : \mathbb{R}^d \times \mathbb{R}^d \rightarrow \mathbb{R} : (x, x') \mapsto \mathbb{E}((g(x) - \mu(x))(g(x') - \mu(x'))^T)$. Most covariance functions contain various hyperparameters, e.g. the Squared Exponential (SE) kernel $k_{SE}(x, x') = \sigma_f^2 \exp(-\frac{(x-x')^2}{2\ell^2})$ contains signal variance σ_f and lengthscale ℓ , which become part of the GP $g_{SE} = \mathcal{GP}(0, k_{SE})$.

¹Code will be published on acceptance

To train the GP hyperparameters, the MLL is the de facto GP loss function, defined as:

$$\log p(y|X, \theta) = -\frac{1}{2}y^T(K + \sigma_n^2 I)^{-1}y - \frac{1}{2}\log|K + \sigma_n^2 I| - \frac{n}{2}\log(2\pi) \quad (1)$$

where $X \in \mathbb{R}^{n \times d}$ and $y \in \mathbb{R}^n$ are a dataset of size n and the GPs hyperparameters θ are hidden in the calculation of the covariance matrix K of observations X .

We refer to all possible parametrizations of GPs with a specific kernel as a *class* of GPs, e.g. all parametrizations of g_{SE} form the class of GPs with the SE kernel.

The set of kernels is closed under various operations (Duvenaud, 2014; Rasmussen & Williams, 2006; Jidling et al., 2017). Among such operations are addition and multiplication of kernels, for example combining a periodic kernel with an squared exponential kernel as $k = k_{PER} \cdot k_{SE}$ enforces locally periodic and smooth behaviour. This grows the set of potentially useful classes of GPs significantly, making model selection a complex endeavour.

2.2. Model Selection for GPs

Model selection tries to find the best model for a dataset (y, X) in terms of accuracy, interpretability or simplicity, preferably all at once. A general rule when selecting models is preferring simpler models that explain the data just good enough, often referred to as Occam’s razor. This should be reflected in model selection criteria, which weigh model performance versus complexity.

Naively, one can use the optimized MLL $\hat{\mathcal{L}} = \log p(y|X, \hat{\theta})$ to assess the model quality for GP g with optimal hyperparameters $\hat{\theta}$. This comes with the downside that increased model complexity allows to (over)fit the data easier and any additional hyperparameter will never decrease the MLL value. Additionally we are solely dependent on the optimization procedure, which might get caught in “bad” optima (cf. Section 4.3). Finally, the MLL is not appropriate for model evaluation under specific conditions, e.g. for m -constant mean functions as discussed in (Karvonen & Oates, 2023).

The performance of a class of GPs can be measured objectively for a dataset through the model evidence (sometimes called marginalized likelihood), i.e. the likelihood marginalized over the hyperparameters θ :

$$\mathcal{Z} = p(y|X) = \int p(y|X, \theta)p(\theta)d\theta \quad (2)$$

Since this integral is intractable one usually resorts to approximations. The most precise approximation to this integral is through sampling based approaches like nested sampling (Skilling, 2006). At its core, the likelihood surface

$p(y|X, \theta)$ is explored by repeatedly sampling hyperparameters from a prior $p(\theta)$. By calculating the weighted sum of those likelihood evaluations, we get a good approximation of the likelihood integral i.e. model evidence \mathcal{Z} . But performing this calculation is often computationally infeasible, even for GPs with two hyperparameters and ten datapoints we need several minutes for this approximation.

Due to this, we look into faster approximations of the likelihood. The earliest is AIC (Akaike, 1974), which is based on the optimized MLL $\hat{\mathcal{L}}$ and corrects the optimum for the number of hyperparameters u as follows: $AIC = 2u - 2\hat{\mathcal{L}}$. It has its roots in information theory and “is derived from a frequentist framework, and cannot be interpreted as an approximation to the model evidence” (cf. p. 162 in (Murphy, 2012)). Related to AIC is BIC, which changes the correction term in dependence to the number of datapoints as $BIC = u \log(n) - 2\hat{\mathcal{L}}$ (Schwarz, 1978), and can be considered a simple approximation to the log model evidence (cf. §5.2.5.1 in (Murphy, 2022)). However, as stated in p. 33 of (Bishop, 2006): “Such criteria do not take account of the uncertainty in the model hyperparameters, however, and in practice they tend to favour overly simple models.”

Most of the methods were applied in various works (Simpson et al., 2021; Kristiadi et al., 2021; Green & Worden, 2015; Ritter et al., 2018; Duvenaud et al., 2013; Lloyd et al., 2014; Hüwel et al., 2021; Härkönen et al., 2023) to approximate different measures with respect to GPs. For example, (Simpson et al., 2021) apply nested sampling to sample from the hyperparameter posterior or (Duvenaud et al., 2013) improve kernel search through BIC.

2.3. Kernel Search Algorithms

The quality and interpretability of a GP model depends strongly on the chosen kernel (Lloyd et al., 2014; Rasmussen & Williams, 2006). While there are commonly used kernels, such as the squared exponential kernel, which works well for generally smooth data, other kernels can provide a better fit for specific kinds of data and allow the inclusion of prior knowledge into the modelling process (Duvenaud, 2014). For example, the periodic and the linear kernel are optimal, if data exhibits periodic and linear behavior, respectively.

In situations without prior knowledge about the data, an automated kernel search algorithm can infer a fitting kernel from the data in an iterative selection process. Introduced with Compositional Kernel Search (CKS) in (Duvenaud et al., 2013; Lloyd et al., 2014), such algorithms construct kernels in an iterative, greedy fashion based on a collection of “base kernels” and operations (e.g. +, ·) w.r.t. some given performance measure, usually the MLL (Hüwel et al., 2021) or BIC (Duvenaud et al., 2013; Lloyd et al., 2014). Many adaptations of those algorithms exist nowadays (Kim & Teh, 2018; Berns et al., 2021; 2022; Hüwel et al., 2022).

Alternative approaches replace the iterative process by learning spectral distributions and model them as a mixture of Gaussians (Li et al., 2019; Wilson & Adams, 2013).

In our experiments, we compare the commonly used performance measures MLL and BIC with AIC, Maximum A Posteriori (MAP) and our Laplace approximations to show their applicability in kernel search.

3. Laplace approximation of GP model evidence

In this section, we detail how to apply the Laplace approximation to approximately solve the model evidence integral in Equation (2). The Laplace approximation $\text{Lap}(f)$ aims to find a Gaussian approximation for a function f using the second order Taylor approximation in log-space of f around its optimum, i.e. a point of gradient equal to zero.

The Laplace approximation has been used in numerous works to train GP hyperparameters or use it to integrate out the latent GP f , instead of the parameters θ , (Li et al., 2023; Flaxman et al., 2015; Kuss & Rasmussen, 2005; Zilber & Katzfuss, 2021; Hartmann & Vanhatalo, 2019). Notable is its applicability to non-Gaussian likelihoods e.g. to optimize hyperparameters for classification GPs and approximate the corresponding marginal likelihood (see chapters 3.4 and 3.5 in (Rasmussen & Williams, 2006)).

In this work we use the Laplace approximation with the goal of computing the model evidence integral in formula (2). Approximating the product $p(y|X, \theta) \cdot p(\theta)$ of likelihood and prior by a second order Taylor approximation in log-space gives us the following:

$$\log \text{Lap}(p(y|X, \theta) \cdot p(\theta)) \approx \log(p(y|X, \hat{\theta}) \cdot p(\hat{\theta})) - \frac{1}{2}(\theta - \hat{\theta})^T H(\theta - \hat{\theta}) \quad (3)$$

Here, $H = -\nabla \nabla \log(p(y|X, \theta) \cdot p(\theta))|_{\theta=\hat{\theta}}$ is the Hessian at a (local) optimum $\hat{\theta}$ (Bishop, 2006), which is easily computed with the autodiff functionality in most ML libraries.

We use the Formula (3) to approximate the integral, resulting in the log model evidence $\log \mathcal{Z}$:

$$\log \mathcal{Z} \approx \log \mathcal{Z}_{\text{Lap}} = \log(p(y|X, \hat{\theta}) \cdot p(\hat{\theta})) + \frac{u}{2} \log(2\pi) \quad (4)$$

$$- \frac{1}{2} \log(|H|) \quad (5)$$

where $\hat{\theta}$ is the optimum found during optimization, u is the number of hyperparameters and H is the Hessian at $\hat{\theta}$. For details of this derivation we refer to Appendix C.1.

Sadly, the next subsection shows that this standard form of Laplace approximation, is not suitable to approximate the model evidence of GPs.

3.1. Overcoming inconsistencies of the Laplace approximation

Naively applying the standard Laplace approximation $\log \mathcal{Z}_{\text{Lap}}$ in formula (4) exhibits an inconsistency, preventing its practical use. In the following we discuss how this inconsistency causes the standard Laplace approximation to increase the model evidence by adding superfluous hyperparameters without necessarily contributing to the model fit. In extreme cases this inconsistency increases the model evidence \mathcal{Z}_{Lap} to infinity, as illustrated in Figure 1 for one dimension. There, a local extremum that is degenerate, in the sense that it is very weak, causes the standard Laplace approximation to result in an infinite model evidence \mathcal{Z}_{Lap} . This directly contradicts Occam’s razor and prevents the usage of the Laplace approximation for approximating the model evidence.

To address this problem, we introduce various versions of the Laplace approximation, all with different interpretations. Doing so, we ensure that the mere presence of a hyperparameter does not contribute to an arbitrary improvement.

The inconsistencies are directly connected to the Hessian H and are best interpreted in one dimension ($u = 1$) after disentangling the dimensions by diagonalizing the Hessian. For hyperparameters where the, one dimensional, Hessian $H = [\lambda]$ is moderately small (e.g. for $\lambda < 1$), we can directly observe from formula (4) that $\frac{1}{2} \log(2\pi) - \frac{1}{2} \log(\lambda)$ has a *positive* contribution to the model evidence just by the hyperparameter of λ *existing*, even without a contribution to the model fit. We therefore modify the Hessian matrix to mitigate this behaviour, similar to Newton methods with Hessian modification in second order optimization (cf. Section 3.4 in (Nocedal & Wright, 1999)).

Lemma 3.1. *To ensure that each hyperparameter of a GP has a minimal negative contribution r in the last to summands of formula (3) to the model evidence \mathcal{Z} , every eigenvalue λ of the Hessian needs to be at least:*

$$\lambda \geq \exp(-2r) \cdot 2\pi \quad (6)$$

For the proof we refer the reader to Appendix C.2.

Based on this equation we suggest three improved variants of the Laplace approximation: *stabilized Laplace* (Lap_0), *AIC corrected Laplace* (Lap_A) and *BIC corrected Laplace* (Lap_B).

Corollary 3.2. *Stabilized Laplace (Lap_0): To ensure a minimal negative contribution $r = 0$ to the log model evidence $\log \mathcal{Z}_{\text{Lap}_0} \approx \log \mathcal{Z}$ every eigenvalue has to be at least $\lambda \geq 2\pi$.*

Corollary 3.3. *AIC corrected Laplace (Lap_A): To ensure a minimal negative contribution $r = -1$ to the model evidence $\log \mathcal{Z}_{\text{Lap}_A} \approx \log \mathcal{Z}$ every eigenvalue has to be at least $\lambda \geq \exp(2) \cdot 2\pi$.*

Corollary 3.4. *BIC corrected Laplace (Lap_B): To ensure a minimal negative contribution $r = -\log(n)$ to the model evidence $\log \mathcal{Z}_{Lap_B} \approx \log \mathcal{Z}$ every eigenvalue has to be at least $\lambda \geq \exp(2 \log(n)) \cdot 2\pi = 2\pi \cdot n^2$.*

Each of the variants has a different interpretation. Stabilized Laplace (Lap_0) prevents additional hyperparameters from improving the model evidence without a significant contribution to the model fit. AIC corrected Laplace (Lap_A) corrects the optimization result similar to AIC by contributing $r = -1$ for each hyperparameter. Finally, BIC corrected Laplace (Lap_B) is correcting similar to BIC by contributing $r = -\log(n)$ for each hyperparameter. The connection to AIC resp. BIC derives from the fact that these corrected Laplace approximations collapse into AIC resp. BIC in the case of all eigenvalues λ of the Hessian being small (see appendix C.3).

These lower bounds for the eigenvalues λ of the Hessian H prevents the inconsistencies model evidence for GP likelihoods. Non-Gaussian likelihoods, also log concave ones like the logistic likelihood in p. 42 in (Rasmussen & Williams, 2006), could also benefit from a similar eigenvalue correction since e.g. log concavity doesn't necessarily prevent infinitely large (or small) likelihood values from superfluous hyperparameters.

4. Evaluation

We demonstrate that our improved variants of the Laplace approximation are superior model selection criteria by comparing them to both the state of the art model selection metrics AIC and BIC and also to MLL and MAP. We use dynamic nested sampling (Higson et al., 2019) to approximate the model evidence, with a precision of up to two decimal places, as our ground truth and perform the following experiments:

1. A comparison of all metrics on a small dataset for a single GP to explore the detailed behaviour of the Laplace approximation and point out the benefits for all metrics in an interpretable way.
2. A kernel search experiment where we vary the selection criteria. Here, the large scale evaluation of models ensures the reproducibility of our results.
3. Comparing all metrics on the Mauna Loa dataset for increasingly more complex kernels to show its applicability on a large and complex real world dataset

Additional details regarding the experiments can be found in their respective appendices under Appendix A. We also detail the normal distributed prior for the hyperparameters we use for nested sampling and our variants of the Laplace approximation in Appendix B.

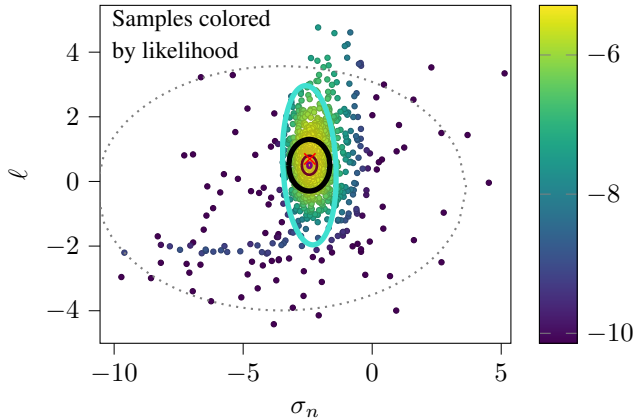


Figure 2. Results of a nested sampling for the linear noisy dataset in Section 4.1 (showing 1024 representative samples out of 12,255 total samples), higher values are better. The differently colored ellipses show the 2σ confidence ellipses for the normal distributions associated with the Laplace approximations for Lap_0 (black), Lap_A (brown), Lap_B (purple) and the standard Laplace approximation (blue). The dotted gray ellipse is the 2σ confidence ellipse for the hyperparameter prior. The \times shows the optimum found during nested sampling. We see that the ellipses derived from our versions of the Laplace approximation give a good approximation of the most relevant area of the likelihood surface, since they cover the majority of the samples of nested sampling.

4.1. Interpretable example

We demonstrate the performance of our Laplace approximations and their similarity to the gold standard, nested sampling, through a detailed exploration of the model evidence and the relevant area of the likelihood surface. We do this for an evenly spaced dataset drawn from a linear function with small noise, and apply an SE-GP containing hyperparameters lengthscale ℓ and noise σ_n (for details see Appendix A.1).

Figure 2 shows the (our versions and standard) Laplace approximations and the samples used to approximate the log model evidence $\log \mathcal{Z}$ during nested sampling. These samples can be interpreted as approximately coming from the hyperparameter posterior. And since we approximate the hyperparameter posterior using the Laplace approximation we can conclude that a high overlap of the samples and the Laplace approximations indicates a high overlap of the relevant area of the likelihood surface. And using the Gaussian interpretation of the Laplace approximation to draw their 2σ confidence ellipses, we can see exactly that. The colored ellipses for the different variants of the Laplace approximation contain 78.4% (standard Laplace in blue), 60.6% (Lap_0 in black), 22.8% (Lap_A in brown) and 3.1% (Lap_B in purple) of the samples (cf. Figure 2). As stabilized Laplace (Lap_0) encircles the majority of the highest valued

Table 1. The ratio of times the data generating kernel was recognized when performing CKS with the respective metric, varied over number of datapoints N . We see that on average, our variants Lap_0 , Lap_A and Lap_B are strong model selection criteria.

N	MLL	AIC	BIC	MAP	LAP_0	LAP_A	LAP_B
5	2.5	42.5	45.0	0.0	42.5	42.5	45.0
10	2.5	47.5	52.5	0.0	47.5	50.0	47.5
20	0.0	65.0	60.0	0.0	55.0	55.0	55.0
30	0.0	60.0	60.0	0.0	55.0	62.5	65.0
40	0.0	60.0	60.0	0.0	62.5	67.5	65.0
50	0.0	57.5	65.0	0.0	62.5	72.5	67.5
100	0.0	60.0	70.0	0.0	67.5	75.0	72.5
200	0.0	70.0	65.0	0.0	75.0	70.0	70.0
AVG.	0.6	57.8	59.7	0.0	58.4	61.9	60.9

points, this again underlines that our variants of the Laplace approximation take the most relevant area of the likelihood surface into account for our approximation. By using stricter negative contributions in our Laplace approximations the corresponding 2σ confidence ellipses for the normal distributions naturally contain fewer and fewer points, which is clearly visible when comparing AIC corrected Laplace (Lap_A , brown) or BIC corrected Laplace (Lap_B , purple) to stabilized Laplace (Lap_0 , black).

In addition to the visual results of Figure 2 showing the similarities of nested sampling and our Laplace approximations, they also show numerical similarities. Nested sampling approximates the log model evidence as $\log \mathcal{Z} = -8.12$ and stabilized Laplace (Lap_0) as $\log \mathcal{Z}_{\text{Lap}_0} = -9.17$. The stricter negative contributions in our Laplace approximations reflect in their log model evidence approximations where AIC corrected Laplace (Lap_A) approximates $\log \mathcal{Z}_{\text{Lap}_A} = -11.17$ and BIC corrected Laplace (Lap_B) as $\log \mathcal{Z}_{\text{Lap}_B} = -13.78$. Interestingly AIC and BIC also provide good results, when rescaling them by -0.5 to live on the same scale as the model evidence, where AIC approximates $\log \mathcal{Z}_{\text{AIC}} = -7.285$ and BIC $\log \mathcal{Z}_{\text{BIC}} = -7.59$. Even though AIC and BIC are similarly close to $\log \mathcal{Z}$, they lack any interpretation comparable to our confidence ellipses and don't allow a diagnosis of overfitting hyperparameters or whether they actually represent the majority of the accepted samples.

4.2. Kernel search experiments

In this experiment we perform the CKS, varying its performance measure between MLL, MAP, AIC, BIC or our three variants of the Laplace approximations. We generate datasets of varying sizes by sampling ten times from four different GPs, for a total of 40 different datasets per dataset size (more details in Appendix A.2). For each dataset-metric combination we perform CKS for, at most, three iterations

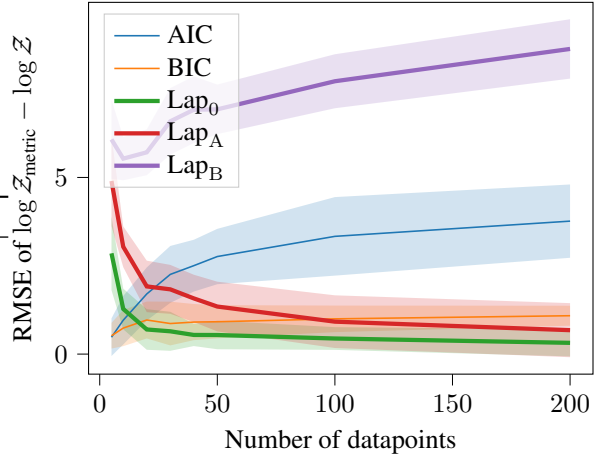


Figure 3. The RMSE \pm one standard deviation, between the log model evidence and the respective metric's value, across varying dataset sizes. AIC and BIC have been rescaled by -0.5 to have the same scale as the model evidence. Smaller RMSE is better. Our variants of the Laplace approximation are drawn in bold.

i.e. resulting kernels contain at most three base kernels. Nested sampling could not be used as a performance measure for CKS due to the large computation time required per model evaluation.

Our variant stabilized Laplace (Lap_0) outperforms the state of the art in its approximation to the model evidence. This is shown in Figure 3 where our approximation to the log model evidence $\log \mathcal{Z}_{\text{Lap}_0}$ reaches an increasingly small distance to the log model evidence $\log \mathcal{Z}$. This distance increases for AIC and BIC for bigger data set sizes, making them unsuitable in practice.

Since stabilized Laplace (Lap_0) approximates $\log \mathcal{Z}$ well, the resulting kernels from the kernel search also have the highest log model evidence, as clearly shown in Table 2. We outperform the state of the art in the important task of finding the kernels with the highest model evidence.

The log likelihoods in Table 3 indicate that our BIC corrected Laplace (Lap_B) exceeds at finding models that work for *different datasets from the same distribution*. This table shows the log likelihood $\log p(y_*|X_*, \theta)$ on a *test dataset* (X_*, y_*), which is *not* the predictive GP likelihood $p(y_*|X_*, y, X, \theta)$, but was calculated by replacing the training datapoints (X, y) with the test datapoints (y_*, X_*) sampled from the same prior GP as the training data. Hence, these resulting kernels represent the original distribution and are flexible enough to model new data from this distribution.

Finally, we show that AIC corrected Laplace (Lap_A) is best at recognizing the underlying data generating model as shown in Table 1. The state of the art, though comparable, is mostly outperformed and we clearly see how MLL and

Table 2. The average log model evidence $\log \mathcal{Z}$, approximated using nested sampling, \pm one standard deviation for models selected during the kernel search experiment. The columns show the results when using the respective metric as the performance measure in CKS. The rows show the number of training datapoints used. Higher values are better and the best performing run w.r.t. the model evidence is bold. The results show that using stabilized Laplace (Lap_0) as the target metric results in kernels with better model evidence.

N	MLL	AIC	BIC	MAP	LAP_0	LAP_A	LAP_B
5	-9.00 ± 2.56	-5.38 ± 3.71	-5.28 ± 3.85	-8.80 ± 2.69	-5.83 ± 4.45	-5.84 ± 4.43	-5.87 ± 4.38
10	-14.12 ± 6.42	-5.37 ± 5.82	-5.72 ± 5.91	-13.90 ± 6.40	-5.32 ± 6.56	-5.46 ± 6.56	-5.63 ± 6.71
20	-23.50 ± 15.63	-2.54 ± 8.94	-3.54 ± 8.52	-23.92 ± 15.90	-1.84 ± 8.91	-2.03 ± 9.04	-2.51 ± 9.12
30	-33.30 ± 26.26	5.25 ± 11.29	4.53 ± 11.45	-33.32 ± 25.28	4.11 ± 11.03	3.84 ± 11.22	3.39 ± 11.37
40	-45.48 ± 37.89	12.33 ± 12.01	12.09 ± 12.03	-40.77 ± 36.68	13.32 ± 11.56	13.09 ± 11.63	12.85 ± 11.78
50	-49.42 ± 48.85	21.14 ± 14.19	21.29 ± 14.54	-48.06 ± 47.07	18.35 ± 12.82	18.02 ± 12.97	17.79 ± 13.10
100	-94.41 ± 100.15	57.92 ± 16.73	57.95 ± 17.10	-89.25 ± 96.13	59.57 ± 18.63	59.50 ± 18.73	59.14 ± 18.73
200	-163.60 ± 196.11	145.34 ± 19.33	146.40 ± 20.86	-189.39 ± 207.50	147.13 ± 20.76	147.06 ± 20.78	146.66 ± 20.63

Table 3. The average log likelihood (normalized by number of datapoints N) on a test dataset \pm one standard deviation for models selected during the kernel search experiment, averaged over the ten test datasets. The test datasets are drawn from the same distributions used to generate the kernel selection datasets. The columns show the results when using the respective metric as the performance measure in CKS. The rows show the number of training datapoints used. Higher values are better and the best performing run w.r.t. the test dataset is bold. The best performing runs are mostly shared between BIC and our BIC corrected Laplace (Lap_B).

N	MLL	AIC	BIC	MAP	LAP_0	LAP_A	LAP_B
5	-1.53 ± 0.56	-3.09 ± 3.67	-2.92 ± 3.48	-1.47 ± 0.51	-1.76 ± 1.57	-1.76 ± 1.57	-1.76 ± 1.57
10	-1.35 ± 0.65	-0.82 ± 1.06	-0.81 ± 1.00	-1.22 ± 0.78	-1.79 ± 3.44	-1.31 ± 1.98	-1.15 ± 1.70
20	-1.34 ± 0.92	-0.10 ± 0.72	0.02 ± 0.55	-1.29 ± 1.05	-3.01 ± 12.41	-2.82 ± 12.39	-0.59 ± 3.51
30	-1.10 ± 0.88	0.20 ± 0.33	0.21 ± 0.33	-1.05 ± 0.88	-0.30 ± 2.45	-0.31 ± 2.45	0.21 ± 0.40
40	-1.16 ± 1.04	0.34 ± 0.28	0.34 ± 0.28	-1.46 ± 1.92	0.23 ± 0.75	0.33 ± 0.31	0.32 ± 0.31
50	-1.46 ± 2.68	-0.12 ± 2.61	-0.12 ± 2.64	-1.21 ± 2.21	-0.16 ± 3.35	-0.16 ± 3.35	-0.09 ± 3.34
100	-1.14 ± 1.16	0.03 ± 3.70	-0.26 ± 4.14	-1.16 ± 1.24	-0.31 ± 4.05	-0.31 ± 4.05	0.58 ± 0.30
200	-0.97 ± 1.04	0.44 ± 1.48	0.22 ± 1.89	-0.95 ± 1.03	0.22 ± 1.87	0.22 ± 1.87	0.73 ± 0.09

MAP tend to result in models of maximal size and thus fail most clearly to recognize the data generating kernels.

These results show how for varying goals, different negative contributions and thus different variants of our Laplace approximations are best fit: Lap_0 for approximating the model evidence, Lap_A for the current dataset, and Lap_B for extrapolation quality. All this while being two orders of magnitude faster than dynamic nested sampling (cf. Figure 4).

Finally, we emphasize the importance of our introduced variants. Here, we just focus on the extreme case of the inconsistency leading to infinite model evidences as in Figure 1. We observed $\log \mathcal{Z}_{\text{Lap}} \approx \pm\infty$, 40.35% of the time. Out of 4884 kernels that were tested during the kernel search, 1971 approximations to the model evidence were completely meaningless. Hence, only our correction to the Laplace approximation made this kernel search experiment possible.

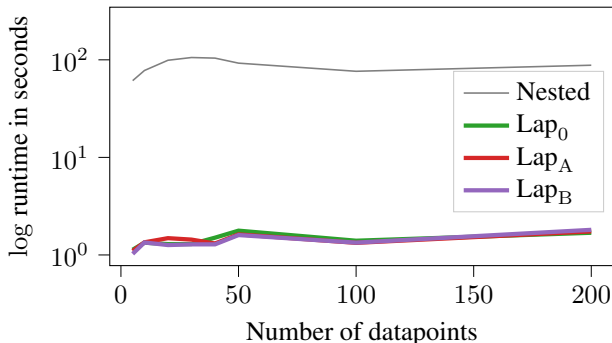


Figure 4. Average time to calculate our metrics, averaged over each kernel evaluated during kernel searches, on a logarithmic scale. For our metrics, the variants of the Laplace approximation, the time includes the training procedure with two random restarts. This shows that the computation time of our approaches are two orders of magnitude smaller than that of dynamic nested sampling.

Table 4. Mauna Loa performance for MLL, MAP, AIC, BIC, our Laplace approximations and the approximated log model evidence $\log \mathcal{Z}$, according to dynamic nested sampling, for the increasingly more sophisticated kernels k_n . We rescale AIC and BIC with -0.5 to be on the same scale as the log model evidence and therefore call them $\log \mathcal{Z}_{AIC}$ and $\log \mathcal{Z}_{BIC}$, here. The approximated log model evidences $\log \mathcal{Z}$ for kernels k_1 through $k_{1+2+3+4}$ have error estimates of ± 3.78 , ± 3.441 , ± 0.29 and ± 5.19 . Higher values indicate that the models are evaluated as better performing.

k	k_1	k_{1+2}	k_{1+2+3}	$k_{1+2+3+4}$
$\log \mathcal{Z}$	-1258.88	-581.45	-293.40	-286.81
LAP_0	-1305.48	-655.84	-288.03	-288.76
LAP_A	-1308.10	-660.84	-295.95	-298.69
LAP_B	-1324.00	-695.87	-348.29	-361.64
$\log \mathcal{Z}_{AIC}$	-1206.85	-554.67	-143.32	-144.09
$\log \mathcal{Z}_{BIC}$	-1213.30	-569.72	-164.83	-169.89
MLL	-1203.85	-547.66	-133.32	-132.08
MAP	-1305.10	-651.77	-285.29	-286.03

4.3. Real world dataset

We conclude the experiments with a discussion of the metrics performance on the Mauna Loa dataset (Keeling & Whorf). We reconstruct the kernel in formula (5.19) of (Rasmussen & Williams, 2006) by iteratively adding its summands as our tested kernels. For each such tested kernel we use AIC, BIC, MLL, MAP, our variants of the Laplace approximations and nested sampling to estimate kernel performance. The summands are k_1 (formula (7)) through k_4 (formula (10)) and we name our tested kernels k_1 through $k_{1+2+3+4}$ to indicate which subkernels they consist of.

$$k_1 = \theta_1^2 \exp\left(-\frac{(x-x')^2}{2\theta_2^2}\right) \quad (7)$$

$$k_2 = \theta_3^2 \exp\left(-\frac{(x-x')^2}{2\theta_4^2} - \frac{2\sin^2(\pi(x-x'))}{\theta_5^2}\right) \quad (8)$$

$$k_3 = \theta_6^2 \left(1 + \frac{(x-x')^2}{2\theta_8\theta_7^2}\right)^{-\theta_8} \quad (9)$$

$$k_4 = \theta_9^2 \exp\left(-\frac{(x-x')^2}{2\theta_{10}^2}\right) + \theta_{11}^2 \delta \quad (10)$$

where δ is the Dirac delta function that is 1 if $x = x'$ and 0 otherwise.

The results in Table 4 show that adding more summands improves performance, which can be expected since each summand was crafted to represent a specific aspect of the dataset. All metrics reflect this behaviour for up to three summands (k_1 through k_{1+2+3}) and also tend to stay very close to the estimated model evidence of nested sampling. Addition of the fourth component, however, is less valued by all metrics (including the approximate model evidence).

Interestingly, in contrast to previous results in Section 4.1 and for kernels k_1 and k_{1+2} , AIC and BIC start to deviate significantly from the approximate log model evidence. This is apparent from the significant overestimation of the log model evidence in columns k_{1+2+3} and $k_{1+2+3+4}$, compared to k_1 and k_{1+2} . We can directly explain this through the value of MLL and the fact that AIC and BIC are derived from it. We see in Table 4 that MLL deviates significantly from the log model evidence which directly affects AIC and BIC. We assume this is due to an unstable optimum, i.e. declining rapidly when deviating from it, which MLL optimization found and AIC/BIC use to represent the model evidence. This problem is less pronounced for the MAP optima since they smooth out such unstable optima via the prior. This stresses the importance of using priors, as is done in our variants of the Laplace approximation.

We conclude that highly complex likelihood surfaces may be at risk of such deviations and suggest using our Laplace approximations there. In any case, an investigation into detecting such unstable optima would be highly beneficial to make more informed metric choices. For example, this behaviour wasn't apparent in Section 4.2. In conclusion this experiment is a clear indicator for the stability of our variants of the Laplace approximation as they do not fail for k_{1+2+3} and $k_{1+2+3+4}$, but further reduce the approximation gap to the log model evidence $\log \mathcal{Z}$.

5. Conclusion

In this paper we introduce novel variants of the Laplace approximation as model selection metrics for GPs. We also provide a method to deal with the inherent inconsistencies of the naive application of the standard Laplace approximation by replacing eigenvalues of the Hessian with varying interpretable thresholds. We show in experiments that our new variants have comparable performance to dynamic nested sampling, which is considered the gold standard in model evidence approximation and that stabilized Laplace (Lap_0) is a good predictor for the model evidence. It further outperforms all other metrics in the kernel search experiment w.r.t. models with the highest model evidence. We further show in that AIC corrected Laplace (Lap_A) resp. BIC corrected Laplace (Lap_B) are best in recognizing the underlying model, used to generate the data, resp. finding models that generalize well to new data from the same distribution. And finally we demonstrate applicability on real world datasets using the Mauna Loa dataset and highlight a weakness of AIC and BIC with respect to optima chosen by MLL.

Acknowledgements

This research was supported by the research training group ‘‘Dataninja’’ (Trustworthy AI for Seamless Problem Solv-

ing: Next Generation Intelligence Joins Robust Data Analysis) funded by the German federal state of North Rhine-Westphalia.

Societal Impact

This paper presents work whose goal is to advance the field of Machine Learning. There are many potential societal consequences of our work, none which we feel must be specifically highlighted here.

References

- Akaike, H. A new look at the statistical model identification. *IEEE transactions on automatic control*, 19(6):716–723, 1974.
- Alvarez, M., Luengo, D., and Lawrence, N. D. Latent force models. In *Artificial Intelligence and Statistics*, pp. 9–16. PMLR, 2009.
- Berns, F., Schmidt, K., Bracht, I., and Beecks, C. 3cs algorithm for efficient Gaussian process model retrieval. In *2020 25th International Conference on Pattern Recognition (ICPR)*, 2021.
- Berns, F., Hüwel, J., and Beecks, C. Automated model inference for gaussian processes: An overview of state-of-the-art methods and algorithms. *SN Computer Science*, 3(4):300, 2022.
- Besginow, A. and Lange-Hegermann, M. Constraining gaussian processes to systems of linear ordinary differential equations. In Oh, A. H., Agarwal, A., Belgrave, D., and Cho, K. (eds.), *Advances in Neural Information Processing Systems*, 2022.
- Bishop, C. M. *Pattern recognition and machine learning*, volume 4. Springer, 2006.
- Borovitskiy, V., Terenin, A., Mostowsky, P., et al. Matérn gaussian processes on riemannian manifolds. *Advances in Neural Information Processing Systems*, 33:12426–12437, 2020.
- Burnham, K. P. and Anderson, D. R. Multimodel inference: understanding aic and bic in model selection. *Sociological methods & research*, 33(2):261–304, 2004.
- Burnham, K. P., Anderson, D. R., Burnham, K. P., and Anderson, D. R. *Practical use of the information-theoretic approach*. Springer, 1998.
- Buyun Liang, T. M. and Sun, J. NCVX: A general-purpose optimization solver for constrained machine and deep learning. 2022.
- Carpenter, B., Gelman, A., Hoffman, M. D., Lee, D., Goodrich, B., Betancourt, M., Brubaker, M. A., Guo, J., Li, P., and Riddell, A. Stan: A probabilistic programming language. *Journal of statistical software*, 76, 2017.

- Duvenaud, D. *Automatic model construction with Gaussian processes*. PhD thesis, University of Cambridge, 2014.
- Duvenaud, D., Lloyd, J., Grosse, R., Tenenbaum, J., and Zoubin, G. Structure discovery in nonparametric regression through compositional kernel search. In *ICML*, 2013.
- Flaxman, S., Wilson, A., Neill, D., Nickisch, H., and Smola, A. Fast kronecker inference in gaussian processes with non-gaussian likelihoods. In *International Conference on Machine Learning*, pp. 607–616. PMLR, 2015.
- Frank E. Curtis, T. M. and Overton, M. L. A BFGS-SQP method for nonsmooth, nonconvex, constrained optimization and its evaluation using relative minimization profiles. *Optimization Methods and Software*, 32(1):148–181, 2017.
- Gardner, J. R., Pleiss, G., Bindel, D., Weinberger, K. Q., and Wilson, A. G. Gpytorch: Blackbox matrix-matrix gaussian process inference with gpu acceleration. In *Advances in Neural Information Processing Systems*, 2018.
- Green, P. L. and Worden, K. Bayesian and markov chain monte carlo methods for identifying nonlinear systems in the presence of uncertainty. *Philosophical Transactions of the Royal Society A: Mathematical, Physical and Engineering Sciences*, 373(2051):20140405, 2015.
- Härkönen, M., Lange-Hegermann, M., and Raiță, B. Gaussian process priors for systems of linear partial differential equations with constant coefficients. *ICML*, 2023.
- Hartmann, M. and Vanhatalo, J. Laplace approximation and natural gradient for gaussian process regression with heteroscedastic student-t model. *Statistics and Computing*, 29(4):753–773, 2019.
- Higson, E., Handley, W., Hobson, M., and Lasenby, A. Dynamic nested sampling: an improved algorithm for parameter estimation and evidence calculation. *Statistics and Computing*, 29:891–913, 2019.
- Holderrieth, P., Hutchinson, M. J., and Teh, Y. W. Equivariant learning of stochastic fields: Gaussian processes and steerable conditional neural processes. In *ICML*, 2021.
- Hüwel, J. D., Berns, F., and Beecks, C. Automated kernel search for gaussian processes on data streams. In *2021 IEEE International Conference on Big Data (Big Data)*, pp. 3584–3588. IEEE, 2021.
- Hüwel, J. D., Haselbeck, F., Grimm, D. G., and Beecks, C. Dynamically self-adjusting gaussian processes for data stream modelling. In *KI 2022: Advances in Artificial Intelligence: 45th German Conference on AI, Trier, Germany, September 19–23, 2022, Proceedings*, pp. 96–114. Springer, 2022.
- Jaynes, E. T. *Probability theory: The logic of science*. Cambridge university press, 2003.
- Jidling, C., Wahlström, N., Wills, A., and Schön, T. B. Linearly constrained Gaussian processes. In *NeurIPS 2017*, 2017.
- Karvonen, T. and Oates, C. J. Maximum likelihood estimation in gaussian process regression is ill-posed. *Journal of Machine Learning Research*, 24(120):1–47, 2023.
- Keeling, C. and Whorf, T. Atmospheric co2 records from sites in the sio air sampling network. *Trends*, 93:16–26.
- Kim, H. and Teh, Y. W. Scaling up the automatic statistician: Scalable structure discovery using gaussian processes. In *International Conference on Artificial Intelligence and Statistics*, pp. 575–584. PMLR, 2018.
- Koposov, S., Speagle, J., Barbary, K., Ashton, G., Bennett, E., Buchner, J., Scheffler, C., Cook, B., Talbot, C., Guillochon, J., Cubillos, P., Ramos, A. A., Johnson, B., Lang, D., Ilya, Dartiailh, M., Nitz, A., McCluskey, A., Archibald, A., Deil, C., Foreman-Mackey, D., Goldstein, D., Tollerud, E., Leja, J., Kirk, M., Pitkin, M., Sheehan, P., Cargile, P., Patel, R., and Angus, R. joshspeagle/dynesty: v2.1.2, June 2023. URL <https://doi.org/10.5281/zenodo.7995596>.
- Kristiadi, A., Hein, M., and Hennig, P. Learnable uncertainty under laplace approximations. In *Uncertainty in Artificial Intelligence*, pp. 344–353. PMLR, 2021.
- Kuss, M. and Rasmussen, C. Assessing approximations for gaussian process classification. *Advances in neural information processing systems*, 18, 2005.
- Lázaro-Gredilla, M., Quiñero-Candela, J., Rasmussen, C. E., and Figueiras-Vidal, A. R. Sparse spectrum gaussian process regression. *JMLR*, 2010.
- Li, C.-L., Chang, W.-C., Mroueh, Y., Yang, Y., and Poczos, B. Implicit kernel learning. In *The 22nd International Conference on Artificial Intelligence and Statistics*, pp. 2007–2016. PMLR, 2019.
- Li, R., John, S., and Solin, A. Improving hyperparameter learning under approximate inference in gaussian process models. *ICML*, 2023.
- Lloyd, J., Duvenaud, D., Grosse, R., Tenenbaum, J., and Ghahramani, Z. Automatic construction and natural-language description of nonparametric regression models. In *Proceedings of the AAAI Conference on Artificial Intelligence*, volume 28, 2014.
- Murphy, K. P. *Machine learning: a probabilistic perspective*. MIT press, 2012.

- Murphy, K. P. *Probabilistic Machine Learning: An introduction*. MIT Press, 2022. URL probml.ai.
- Nocedal, J. and Wright, S. J. *Numerical optimization*. Springer, 1999.
- Rasmussen, C. E. and Williams, C. K. *Gaussian processes for machine learning*, volume 2. MIT press Cambridge, MA, 2006.
- Ritter, H., Botev, A., and Barber, D. Online structured laplace approximations for overcoming catastrophic forgetting. *Advances in Neural Information Processing Systems*, 31, 2018.
- Schwarz, G. Estimating the dimension of a model. *The annals of statistics*, pp. 461–464, 1978.
- Simpson, F., Lalchand, V., and Rasmussen, C. E. Marginalised gaussian processes with nested sampling. *Advances in neural information processing systems*, 34: 13613–13625, 2021.
- Skilling, J. Nested sampling for general bayesian computation. 2006.
- Speagle, J. S. DYNESTY: a dynamic nested sampling package for estimating Bayesian posteriors and evidences. *Monthly Notices of the Royal Astronomical Society*, 493 (3):3132–3158, April 2020. doi: 10.1093/mnras/staa278.
- Wilson, A. and Adams, R. Gaussian process kernels for pattern discovery and extrapolation. In *International conference on machine learning*, pp. 1067–1075. PMLR, 2013.
- Zilber, D. and Katzfuss, M. Vecchia–laplace approximations of generalized gaussian processes for big non-gaussian spatial data. *Computational Statistics & Data Analysis*, 153:107081, 2021.

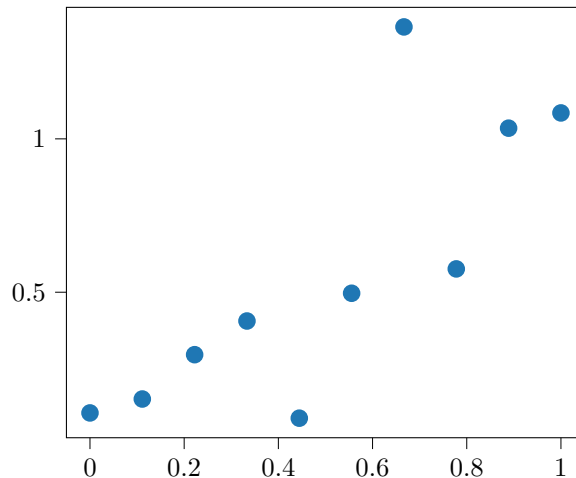


Figure 5. The dataset used in the first experiment. Ten datapoints $y = x + \sigma_n$ at evenly distributed locations $x = 0 \dots 1$ with $\sigma_n \sim \mathcal{N}(0, 0.1)$

Appendices

A. Additional experiment details

If not otherwise specified we use the following settings in our experiments:

We use GPyTorch’s (Gardner et al., 2018) implementation for GPs.

GP training was performed using PyGRANSO (Buyun Liang & Sun, 2022), a Python port of the GRANSO (Frank E. Curtis & Overton, 2017) optimizer with either MLL loss for MLL, AIC and BIC or MAP loss for MAP and our Laplace approximations. The training using PyGRANSO was repeated five times, randomly reinitializing the GP every time, for at most 1000 iterations every training.

We estimate our ground truth model evidence \mathcal{Z} with dynamical nested sampling (Higson et al., 2019) using the dynesty library (Koposov et al., 2023; Speagle, 2020) with standard settings, i.e. automatic sampler selection, multi bounds and automatic live point selection until the the improvement to the model evidence is less than 0.01 (i.e. $d\log z < 0.01$). The hyperparameter prior used in nested sampling is constructed from the priors discussed in Appendix B.

A.1. INTERPRETABLE EXPERIMENT

We used the linear dataset shown in Figure 5. The tested GP was a standard Squared Eponential (SE) GP with an additional noise hyperparameter.

A.2. KERNEL SEARCH EXPERIMENT

In the kernel search experiment we perform CKS with depth three, i.e. kernels can have at most three elements. The set of base kernels for CKS contains the SE kernel, the linear kernel and the Matérn 3/2 kernel. The kernels are not scaled with additional coefficients σ_f . But all GP models have a noise hyperparameter σ_n added to the diagonal. The allowed operations are addition and multiplication.

The datasets used are generated by sampling ten datasets from four different GPs. These GPs are standard initializations of GPyTorch GPs with kernels Linear, SE, Matérn 3/2 and SE+SE. For each of these 40 datasets, a kernel search was performed, for each metric. We generated datasets with 5, 10, 20, 30, 40, 50, 100 and 200 datapoints.

The approximated model evidence \mathcal{Z} was calculated for the resulting kernel chosen by CKS.

For the calculation of the likelihood for test datasets, we sample another ten datasets from the same GPs used to generate the training data. This ensures, that they come from the same distribution. For each such dataset we then calculate the MLL by

Table 5. The determined means and standard deviations for the hyperparameters of used kernels.

Kernel	Hyperparameter	Mean	Standard deviation
squared exponential	lengthscale	-0.212	1.89
Matérn 3/2	lengthscale	0.8	2.15
periodic	lengthscale	0.78	2.29
	period length	0.65	1.0
rational quadratic	lengthscale	-0.05	1.94
	alpha	1.88	3.1
linear	variance	-0.8	1.0
scale kernel	σ_f	-1.63	2.26
noise	σ_n	-3.52	3.58

replacing the training dataset with the test dataset, without retraining the model.

A.3. MAUNA LOA EXPERIMENT

In this setting we added an additional stopping criterion for the dynamical nested sampling, stopping after at most three million (3000000) samples to cap runtime.

B. Choosing the hyperparameter prior

The normal distributed prior was selected by training GPs with various kernels on randomly generated data from various GPs. Training was performed on data normalized to zero mean and one standard deviation, to make it consistent for the experiments. All GPs were trained on data from all other GPs, e.g. a periodic kernel trained on data generated by a Matérn kernel, squared exponential kernel, etc. Hyperparameters are stored in their raw form, i.e. before applying the `Positive` constraint from GPyTorch. In particular, the hyperparameter priors are applied to the raw form. The priors for the scaling hyperparameter σ_f and the noise σ_n are based on training results of *all* kernels. Show the hyperparameter priors for the raw values in Table 5. All our priors are normal distributions with diagonal covariances. To construct the prior $p(\theta) \sim \mathcal{N}(\theta_\mu, \Sigma)$ for a specific GP with kernel k we concatenate the respective means and squared standard deviations from Table 5 to construct the vector θ_μ and the diagonal matrix Σ .

The choice of these hyperparameter priors is *not* the main reason for the superiority of our variants of the Laplace approximation over AIC and BIC, as otherwise MAP would benefit from these hyperparameter priors. Clearly, the experiments show, that MAP is not a good model selection criteria.

C. Laplace approximation derivations

We derive the various Laplace approximations for the model evidence $p(y|X) = \int_\theta p(y|X, \theta) \cdot p(\theta) d\theta$ with likelihood $p(y|X, \theta)$ and prior $p(\theta)$ for GP hyperparameters θ .

C.1. LAP

We start with the application of the standard Laplace approximation.

$$\begin{aligned}
 f(\theta) &= p(y|X, \theta) \cdot p(\theta) \\
 \log(f(\theta)) &= \log(p(y|X, \theta)) \cdot p(\theta) \\
 \log(f(\theta)) &\approx \log(f(\hat{\theta})) - \frac{1}{2}(\theta - \hat{\theta})H(\theta - \hat{\theta})^T \\
 f(\theta) &\approx f(\hat{\theta}) \exp\left(-\frac{1}{2}(\theta - \hat{\theta})H(\theta - \hat{\theta})^T\right)
 \end{aligned}$$

where $H = -\nabla\nabla \log f(\theta)$. We then insert the approximation into the model evidence integral.

$$p(y|X) = \int_{\theta} f(\theta) d\theta \quad (11)$$

$$\approx f(\hat{\theta}) \cdot \int_{\theta} \exp\left(-\frac{1}{2}(\theta - \hat{\theta})H(\theta - \hat{\theta})^T\right) d\theta \quad (12)$$

$$= f(\hat{\theta}) \cdot \frac{(2\pi)^{-\frac{u}{2}} \cdot |H^{-1}|^{-\frac{1}{2}}}{(2\pi)^{-\frac{u}{2}} \cdot |H^{-1}|^{-\frac{1}{2}}} \int_{\theta} \exp\left(-\frac{1}{2}(\theta - \hat{\theta})H(\theta - \hat{\theta})^T\right) d\theta \quad (13)$$

$$= f(\hat{\theta}) \cdot \frac{1}{(2\pi)^{-\frac{u}{2}} \cdot |H^{-1}|^{-\frac{1}{2}}} \int_{\theta} (2\pi)^{-\frac{u}{2}} \cdot |H^{-1}|^{-\frac{1}{2}} \exp\left(-\frac{1}{2}(\theta - \hat{\theta})H(\theta - \hat{\theta})^T\right) d\theta \quad (14)$$

$$= f(\hat{\theta}) \cdot \frac{1}{(2\pi)^{-\frac{u}{2}} \cdot |H^{-1}|^{-\frac{1}{2}}} \cdot 1 \quad (15)$$

$$\log(p(y|X)) \approx \log(f(\hat{\theta})) + \frac{u}{2} \log(2\pi) + \frac{1}{2} \log(|H^{-1}|) \quad (16)$$

$$\log(p(y|X)) \approx \widehat{\mathcal{L}}_{\text{MAP}} + \frac{u}{2} \log(2\pi) + \frac{1}{2} \log(|H^{-1}|) \quad (17)$$

$$\log(p(y|X)) \approx \widehat{\mathcal{L}}_{\text{MAP}} + \frac{u}{2} \log(2\pi) - \frac{1}{2} \log(|H|) \quad (18)$$

where u is the number of hyperparameters. This leaves us with our approximation for the model evidence based on the log MAP and the remaining correction term.

C.2. PROOF OF LEMMA 3.1

Due to the discussed pathologies of the Laplace approximation we replace some eigenvalues λ of the Hessian H with values based on minimal negative correction terms r . We start with the approximation in formula (18) and want to have a minimal negative correction value of r for the term $+\frac{u}{2} \log(2\pi) - \frac{1}{2} \log(|H|)$. We motivated this approach during the discussion of Laplace approximations pathologies in section 3.1. Again, in one dimension it holds that if a hyperparameter is superfluous, the likelihood surface will be mostly independent of it and, in the extreme, constant in its direction. Thus, we correct the Hessian in those directions by replacing its eigenvalues.

Proof. Lemma 3.1 Diagonalize the Hessian H using the (orthogonal) matrix T of eigenvectors to $\Lambda = THT^{-1}$, where Λ is a diagonal matrix of eigenvalues. Then, due to the determinant formula $|H| = |T||H||T^{-1}| = |\Lambda|$, we reduce to the case of a one-dimensional (i.e. $u = 1$) inequality. Writing $\Lambda = [\lambda]$ we get:

$$\begin{aligned} & r \geq \frac{1}{2} \log(2\pi) - \frac{1}{2} \log(\lambda) \\ \iff & 2r \geq \log(2\pi) - \log(\lambda) \\ \iff & -2r + \log(2\pi) \leq \log(\lambda) \\ \iff & \exp(-2r + \log(2\pi)) \leq \lambda \\ \iff & \exp(-2r)2\pi \leq \lambda \end{aligned}$$

This is our intended result. □

C.3. PROOF OF LAP COLLAPSING INTO AIC/BIC

Here we show that, in the case that all eigenvalues λ of H are small (i.e. they are all replaced with the lower bound), our approximation collapses into MAP or AIC resp. BIC with MAP as a surrogate for the likelihood function.

$$\begin{aligned}
 \log(p(y|X)) &\approx \widehat{\mathcal{L}}_{MAP} + \frac{u}{2} \log(2\pi) - \frac{1}{2} \log(|H|) \\
 \iff \log(p(y|X)) &\approx \widehat{\mathcal{L}}_{MAP} + \frac{u}{2} \log(2\pi) - \frac{1}{2} \log\left(\prod_{i=1}^u 2\pi \cdot \exp(-2r)\right) \\
 \iff \log(p(y|X)) &\approx \widehat{\mathcal{L}}_{MAP} + \frac{u}{2} \log(2\pi) - \frac{1}{2} \sum_{i=1}^u \log(2\pi \cdot \exp(-2r)) \\
 \iff \log(p(y|X)) &\approx \widehat{\mathcal{L}}_{MAP} + \frac{u}{2} \log(2\pi) - \frac{u}{2} \log(2\pi \cdot \exp(-2r)) \\
 \iff \log(p(y|X)) &\approx \widehat{\mathcal{L}}_{MAP} + \frac{u}{2} \log(2\pi) - \frac{u}{2} \log(2\pi) + ur \\
 \iff \log(p(y|X)) &\approx \widehat{\mathcal{L}}_{MAP} + ur
 \end{aligned}$$

Now inserting our values for the minimal correction $r = 0$, $r = -1$ and $r = -\log(n)$ we get back $\log(p(y|X)) \approx \widehat{\mathcal{L}}_{MAP}$, $\log(p(y|X)) \approx \widehat{\mathcal{L}}_{MAP} - u$ and $\log(p(y|X)) \approx \widehat{\mathcal{L}}_{MAP} - u \cdot \log(n)$, which are just $-\frac{1}{2}$ AIC resp. $-\frac{1}{2}$ BIC when choosing $\widehat{\mathcal{L}} = \widehat{\mathcal{L}}_{MAP}$ for AIC resp. BIC.

D. Licences

GPpyTorch (Gardner et al., 2018) and Dynesty (Koposov et al., 2023; Speagle, 2020) are both licensed under the MIT license (<https://github.com/cornellius-gp/gpytorch/blob/master/LICENSE>, <https://github.com/joshspeagle/dynesty/blob/31b7e61031330ecb0b6df937b4013d8d592a6755/LICENSE>).

E. Reproducibility

For reproducibility we store the seeds used in the kernel search experiments.

F. Compute

All training was performed on a server with an Intel(R) Core(TM) i9-10900K CPU @ 3.70GHz and 64GB of RAM.